



Effects of H₂ ambient annealing in fully 0 0 2-textured ZnO:Ga thin films grown on glass substrates using RF magnetron co-sputter deposition

Sungyeon Kim^a, Jungmok Seo^b, Hyeon Woo Jang^c, Jungsik Bang^c, Woong Lee^d, Taeyoon Lee^b, Jae-Min Myoung^{a,*}

^a Information and Electronic Materials Research Laboratory, Department of Materials Science and Engineering, Yonsei University, 134 Shinchon-Dong, Seodaemun-Gu, Seoul 120-749, Republic of Korea

^b Nanobio Fusion Device Laboratory, School of Electrical and Electronic Engineering, Yonsei University, 134 Shinchon-Dong, Seodaemun-Gu, Seoul 120-749, Republic of Korea

^c LG Chem, Ltd./Research Park, 104-1 Moonji-Dong, Yuseng-Gu, Daejeon 305-380, Republic of Korea

^d School of Nano & Advanced Materials Engineering, Changwon National University, 9 Sarim-dong, Changwon, Gyeongnam 641-773, Republic of Korea

ARTICLE INFO

Article history:

Received 4 October 2008

Received in revised form 30 November 2008

Accepted 30 November 2008

Available online 7 December 2008

PACS:

42.79.–e

61.72.–y

68.37.Hk

68.37.Ps

68.55.–a

68.55.Ln

73.61.–r

78.20.–e

81.15.Cd

82.80.–d

Keywords:

Doping (A1)

X-ray diffraction (A1)

Physical vapor deposition processes (A3)

Gallium compounds (B1)

Zinc compounds (B1)

Semiconducting materials (B2)

ABSTRACT

Gallium doped zinc oxide (ZnO:Ga) thin films were grown on glass substrates using RF magnetron co-sputtering, followed by H₂ ambient annealing at 623 K to explore a possibility of steady and low-cost process for fabricating transparent electrodes. While it was observed that the ZnO:Ga thin films were densely packed *c*-axis oriented self-textured structures, in the as-deposited state, the films contained Ga₂O₃ and ZnGa₂O₄ which had adverse effect on the electrical properties. On the other hand, post-annealing in H₂ ambient improved the electrical properties significantly via reduction of Ga₂O₃ and ZnGa₂O₄ to release elemental Ga which subsequently acted as substitutional dopant increasing the carrier concentration by two orders of magnitude. Transmittance of the ZnO:Ga thin films were all over 90% that of glass while the optical band gap varied in accordance with the carrier concentrations due to changes in Fermi level. Experimental observation in this study suggests that transparent conductive oxide (TCO) films based on Ga doped ZnO with good electrical and optical properties can be realized via simple low-cost process.

© 2008 Elsevier B.V. All rights reserved.

1. Introduction

Transparent conductive oxide (TCO) thin films, of which the representative material is the indium tin oxide (ITO), have been widely used in transparent electrodes for flat panel displays, solar cells, and organic light-emitting diodes due to the high luminous transmittance, good electrical conductivity, superior adhesion to substrate, and chemical inertness [1–5]. Due to the high cost in raw materials of indium, however, zinc oxide (ZnO) thin films with *n*-type dopants including Al, Ga, In, and B have been extensively

studied to be an alternative to ITO. As previously reported, Al doped ZnO (ZnO:Al) thin films show good transparent and conducting properties whose resistivity has achieved the order of $1 \times 10^{-4} \Omega \text{ cm}$ with average transparency of more than 85% in visible regions [6–8]. Despite of the superior properties of ZnO:Al as a replacement for TCO, it shows relatively low thermal stability and degeneration problem in long time exposure to air ambient originated from high reactivity of aluminum [9,10].

Recently, gallium as a dopant in ZnO has drawn great attentions due to low reactivity and more resistant characteristics to oxidation compared to aluminum. In addition, slightly smaller bond length of Ga–O (1.92 Å) than that of Zn–O (1.97 Å) allows higher solubility of Ga in ZnO matrix leading to the high flexibility in doping concentration [11]. Thus, it is considered that

* Corresponding author. Tel.: +82 2 2123 2843; fax: +82 2 365 2680.

E-mail address: jmmyoung@yonsei.ac.kr (J.-M. Myoung).

ZnO:Ga-based TCOs are relatively inexpensive while they have desirable properties besides electrical and optical properties such as non-toxicity, long-term environmental stability and excellent infrared (IR) shielding which are not easily obtained in ZnO:Al [12–14].

Published electrical resistivity, carrier concentration, mobility, and optical transmittance of polycrystalline ZnO:Ga thin films range from 2.58×10^{-2} to $1.4 \times 10^{-4} \Omega \text{ cm}$, 5.28×10^{19} to $5.51 \times 10^{21} \text{ cm}^{-3}$, 0.669 to $54.2 \text{ cm}^2/\text{Vs}$, and approximately 70 to well above 90%, respectively [15–17]. Excellent electrical and transparent properties of high crystalline ZnO:Ga thin films grown on single crystal substrates had been reported [16,18,19]. Bhosle achieved the lowest resistivity of $1.4 \times 10^{-4} \Omega \text{ cm}$ with (002) epitaxial ZnO:Ga thin films grown on sapphire by pulsed laser deposition (PLD) [16]. Park et al. reported that high quality ZnO:Ga thin film deposited by PLD on quartz substrate at 573 K shows a low electrical resistivity of $8.12 \times 10^{-5} \Omega \text{ cm}$, a carrier concentration of $1.46 \times 10^{22} \text{ cm}^{-3}$, and a carrier mobility of $30.96 \text{ cm}^2/\text{Vs}$ with a visible transmittance of above 90% [18]. These large differences on electrical property are presumably due to corresponding variations in film composition, microstructure, deposition technique, and post-deposition process.

In this article, we studied the growth characteristics and properties of ZnO:Ga thin films on glass substrate by varying growth temperature ranging from room temperature (RT) to 623 K, focusing on the effect of subsequent H_2 ambient annealing on the electrical, structural, and optical properties. Among various deposition techniques, RF magnetron sputtering system was chosen due to its advantageous features such as simple apparatus, high deposition rates, and low deposition temperature. Particularly, with the potential controllability of the dopant concentrations in mind, dual target co-deposition system was used. It was demonstrated that in despite of initially poor electrical properties due to the formation of undesirable oxides phases, once post-annealed in hydrogen at relatively low temperature, the ZnO:Ga thin films showed significant improvement in electrical properties ensuring that it is a promising potential ITO substitute that can be produced with relatively simple process.

2. Experimental procedure

The transparent conductive ZnO:Ga thin films were deposited on glass substrates by RF magnetron co-sputtering using ZnO (99.99%) and Ga_2O_3 (99.9%) targets by varying deposition temperature (T_s) from RT to 623 K. Glass substrates, cleansed via a standard cleaning procedure, was loaded in the central region of the substrate holder located about 50 mm away from the target. The sputtering chamber was initially evacuated to a base pressure of $\sim 5.1 \times 10^{-4} \text{ Pa}$ and the working pressure was maintained at $\sim 7.3 \times 10^{-1} \text{ Pa}$ with an Ar ambient gas (99.999%). The RF power of the ZnO and Ga_2O_3 target were fixed at 150 and 75 W, respectively, to deposit in the transparent conductive films for 20 min. As-deposited thin films, after initial characterizations, were annealed in H_2 ambient at 623 K for an hour. The thicknesses of films were determined by cross-sectional scanning electron microscopy (SEM). The surface morphology and the crystalline characteristics of thin films were investigated by atomic force microscopy (AFM, Digital Instruments Nanoscope II) and X-ray diffraction (XRD), respectively. Ga concentration in ZnO film was determined by energy dispersive X-ray spectroscopy (EDS). The chemistry of transparent conductive ZnO:Ga thin films were studied using X-ray photoelectron spectroscopy (XPS). The electrical properties of the ZnO:Ga thin films were measured at room temperature by van der Pauw method. The optical properties of ZnO:Ga thin films were examined using UV–vis spectrophotometer.

3. Results and discussion

Morphology of the ZnO:Ga thin films were evaluated first before the discussion of their electrical and optical properties since the effect of the morphology-related factors on these properties could not be neglected. Fig. 1 shows the SEM images of the as-deposited and post-annealed films for the deposition temperatures of 298, 373, 473, and 623 K, respectively. The films thicknesses estimated from the cross-sectional images (not shown) varied slightly from 420 to 450 nm and these values did not change after the post-annealing treatment in hydrogen. Further, in Fig. 1, it can be seen that all the films have densely packed columnar grain structures, implying the textured growth of the films along a specific crystallographic orientation.

Regarding the surface roughness, Fig. 2 shows that the roughness estimated from the AFM observations (image not shown) increases with higher deposition temperature (from 7.9 to 12.7 nm) in the as-deposited state. It is well known that higher deposition temperature yields increased surface roughness of the ZnO thin films [20] and the ZnO:Ga thin films herein also show the same trend. It is also seen in Fig. 2 that there is no noticeable change in the roughness after the hydrogen annealing treatment (7.5–11.1 nm). As the surface roughness increases, it is more likely that negatively charged oxygen-related species are adsorbed on the surface of the crystallites which in turn act as electron traps [21]. At the same time, the rough surface scatters the incident light beam to reduce the optical efficiencies. However, since the change in the surface roughness is somewhat small with the varying deposition temperature and with the post-annealing treatment, it can be said that the effect of the changes in surface roughness accompanying the processing conditions on electrical and optical properties of ZnO:Ga thin films could be excluded in this study.

Apart from the morphology, crystallinity could also affect the electrical and optical properties of the ZnO:Ga thin films. Therefore, the XRD spectra of the ZnO:Ga thin films shown in Fig. 3 are examined. In the XRD spectra for the as-deposited samples shown in Fig. 3(a), most prominent peaks at the Bragg angle of about 34.3° are assigned to ZnO (002) while those at 36.3° , 47.7° and 62.8° are to ZnO (101). Together with this, the intensities of these ZnO (002) peaks tend to increase with higher deposition temperature whereas those for ZnO (102) and (103) decrease. It is therefore deduced that the ZnO:Ga thin films all have the preferred c-axis orientation due to self-texturing regardless of the deposition temperature and that the crystallinity would be improved when the growth temperature is increased from RT. Decrease in the intensity of the ZnO (101) peaks also suggest that rather random nucleation of ZnO crystallites due to the role of Ga providing nucleation sites [22] is suppressed when higher deposition temperature is employed.

One interesting feature noticed in Fig. 3(a) is the presence of the diffraction peaks due to other oxide phases. While the peak at 43.7° is assigned to ZnGa_2O_4 (400), the 37.5° peak can be assigned to both Ga_2O_3 (401) and ZnGa_2O_4 (222). Similarly, the 57.5° peak can be assigned to both Ga_2O_3 ($\bar{3}13$) and ZnGa_2O_4 (511). Peaks related to Ga_2O_3 tend to decrease as the deposition temperature is increased; however, that due to ZnGa_2O_4 remain almost similar regardless of the deposition temperature. These changes in the XRD peak intensities suggest that Ga is supplied in the form of Ga_2O_3 from the sputtering target and incorporated into the ZnO phase as clusters without full decomposition at low deposition temperature. Increasing the processing temperature then provide sufficient thermal energy for the dissociation of Ga_2O_3 . Presence of the ZnGa_2O_4 peaks indicates that some Ga_2O_3 species from one sputtering target can combine with ZnO species from the other target stoichiometrically to form spinel structure. It was reported that when Ga concentration exceeds the solubility limit in ZnO:Ga

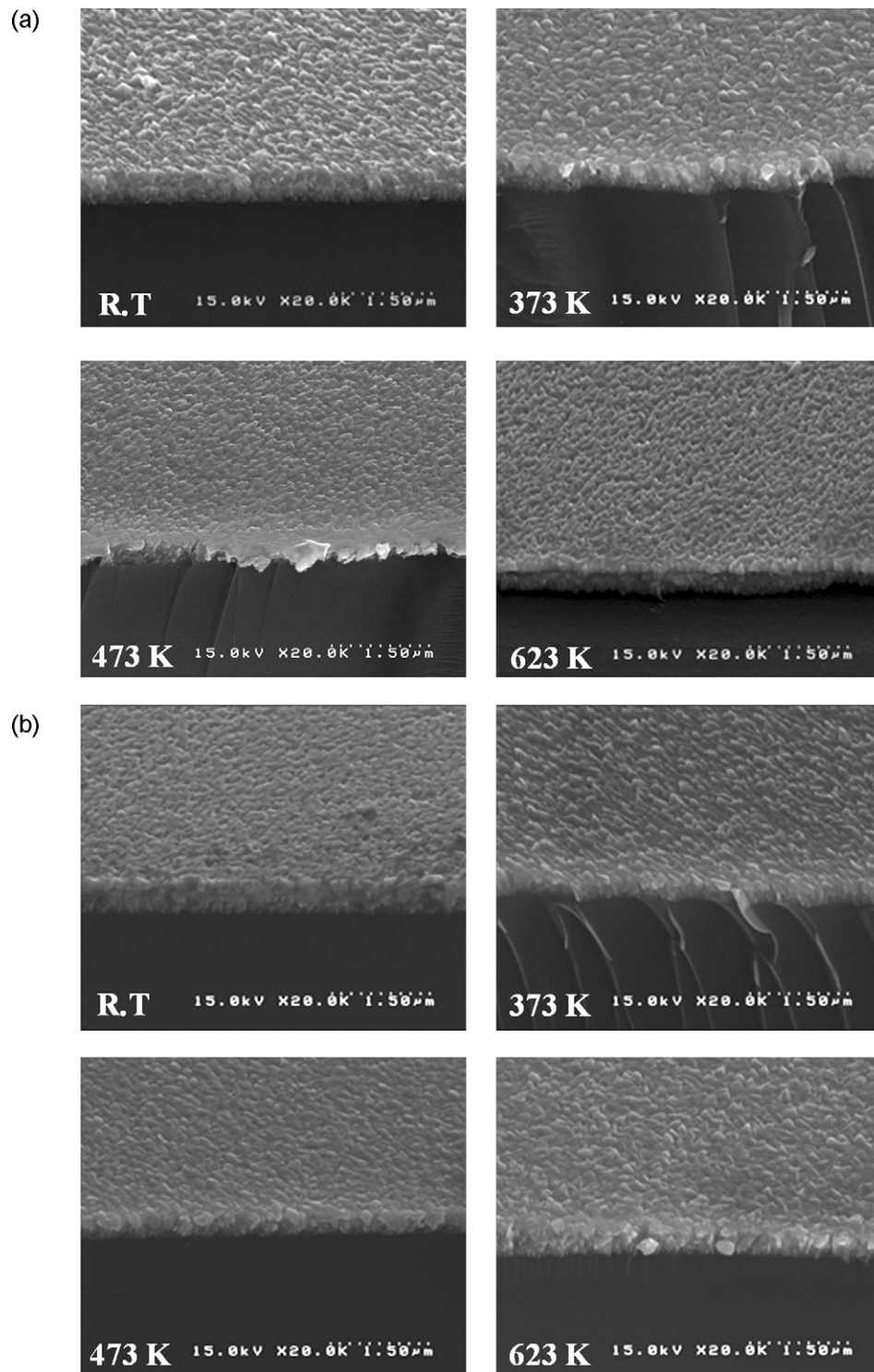


Fig. 1. SEM micrographs showing the surface and cross-section for the (a) as-deposited and (b) post-annealed ZnO:Ga thin films deposited at various temperatures.

thin film, which is known to be about 2.32 at%, ZnGa_2O_4 phase can be formed [23]. In this regard, relative insensitivity of the ZnGa_2O_4 peaks to the deposition temperature in intensities also means that the ZnO:Ga thin films in this study contain Ga in excess of the solubility limit. Indeed, the Ga concentrations of the films estimated from the EDS were about 3.5 ± 0.3 at%. These observations and inferences suggest that in as-doped state, these ZnO:Ga thin films would show relatively poorer electrical properties. First, with its band gap energy of 4.4 eV, Ga_2O_3 insulator phase would provide traps for conduction electrons [24]. Further, in the spinel structure of

ZnGa_2O_4 , Ga^{3+} ions occupy the non-substitutional sites with octahedral symmetry and these non-substitutional Ga will have no contribution of conduction electron considering that the band gap energy of ZnGa_2O_4 is about 5.0 eV [25].

Once the as-deposited ZnO:Ga thin films were post-annealed in H_2 ambient, their crystallinity underwent significant changes as seen in Fig. 3(b). In the XRD spectra of the post-annealed samples, peaks attributed to Ga_2O_3 are nearly vanished and those due to ZnGa_2O_4 remain only in the sample initially deposited at 473 K with their intensities substantially decreased. Disappearance of

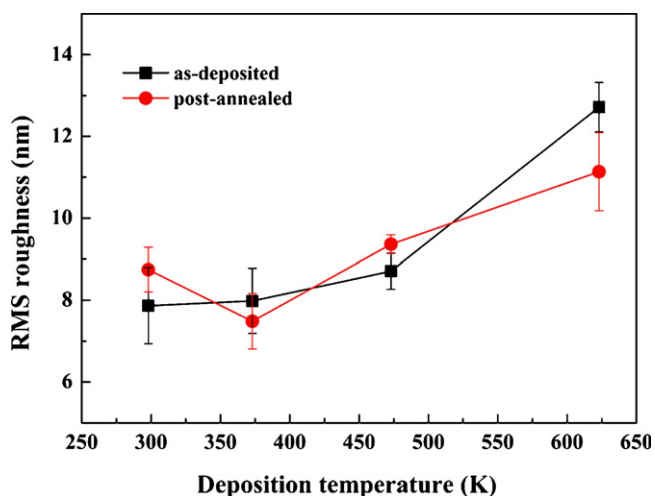


Fig. 2. Root mean square (RMS) roughness (estimated from the AFM observations) of the ZnO:Ga thin films deposited at various temperatures.

the Ga_2O_3 and ZnGa_2O_4 peaks implies that the post-annealing treatment in H_2 ambient has decomposed these oxide phases leaving isolated Ga atoms that would subsequently diffuse into the ZnO lattice to substitute Zn atoms or to occupy interstitial positions. This presumption is supported by the shifted ZnO (0 0 2) peaks to lower diffraction angles (about 34.1°), i.e. increased interplanar distance along c -axis, in Fig. 3(b). It may be argued that the post-annealing treatment itself caused such changes in the crystalline structure by providing thermal energy for the non-substitutional Ga atoms to occupy the substitutional sites. However, noting that the intensities of the Ga_2O_3 and ZnGa_2O_4 peaks for the as-deposited films do not vary noticeably with the deposition temperature [Fig. 3(a)], it is more likely that hydrogen played the role of reducing agent in the current study. As for the

small traces of the Ga_2O_3 and ZnGa_2O_4 peaks for the sample initially deposited at 473 K, it is presumed that the specific deposition condition allowed the circumstances for the formation of the most stable microstructure composed of ZnO, Ga_2O_3 and ZnGa_2O_4 so that even the hydrogen treatment was not sufficient to eliminate the oxide phases completely.

Fig. 4(a)–(h) shows the representative XPS spectra at different growth temperatures ranging from RT to 623 K for both as-deposited and post-annealed samples, which supports above discussion on the XRD results. The uniform distribution of Ga in film within the instrumental uncertainty was confirmed by depth profile of XPS (not shown) using Ar ion gun sputtering, of which qualitative values is in good agreement with previous EDS results. In the XPS spectra for the as-deposited films [Fig. 4(a)–(d)], peaks at about 1117 and 1143 eV are attributed to Ga $2p_{3/2}$ and Ga $2p_{1/2}$, respectively implying that Ga exists in the as-deposited films as Ga^{3+} [26]. However, as seen in the XRD spectra in Fig. 3(a), there exist Ga_2O_3 and ZnGa_2O_4 , in which Ga is in Ga^{3+} state. Therefore, it is evident that not all Ga substituted Zn in the ZnO lattice. Further, in Fig. 4(a)–(d), numerous small peaks can be observed, which may indicate that some of the dopant Ga is not in chemically stable states. After having undergone the post-annealing treatment in hydrogen, the XPS spectra has changed significantly as seen in Fig. 4(e)–(h). Now, the Ga $2p_{3/2}$ and Ga $2p_{1/2}$ peaks at 1116 and 1143 eV positions are more intense as compared to other sub-peaks or background noises. Together with the XRD spectra in Fig. 3(b) in which peaks from the secondary oxide phases almost vanished, this indicates that Ga in Ga^{3+} state is incorporated in the ZnO lattice by substituting the Zn sites. One interesting feature in Fig. 4(e)–(h) is that there are small satellite peaks or shoulders in the lower binding energy side of Ga $2p_{3/2}$ peaks (marked with arrows) located at 1114 eV positions, i.e. 2 eV lower than Ga $2p_{3/2}$ peaks, which are attributed to the presence of elemental Ga [23]. This could be regarded as evidence that Ga_2O_3 and ZnGa_2O_4 initially present in the as-deposited state are reduced by the post-annealing in hydrogen to release Ga atoms and these Ga cannot be

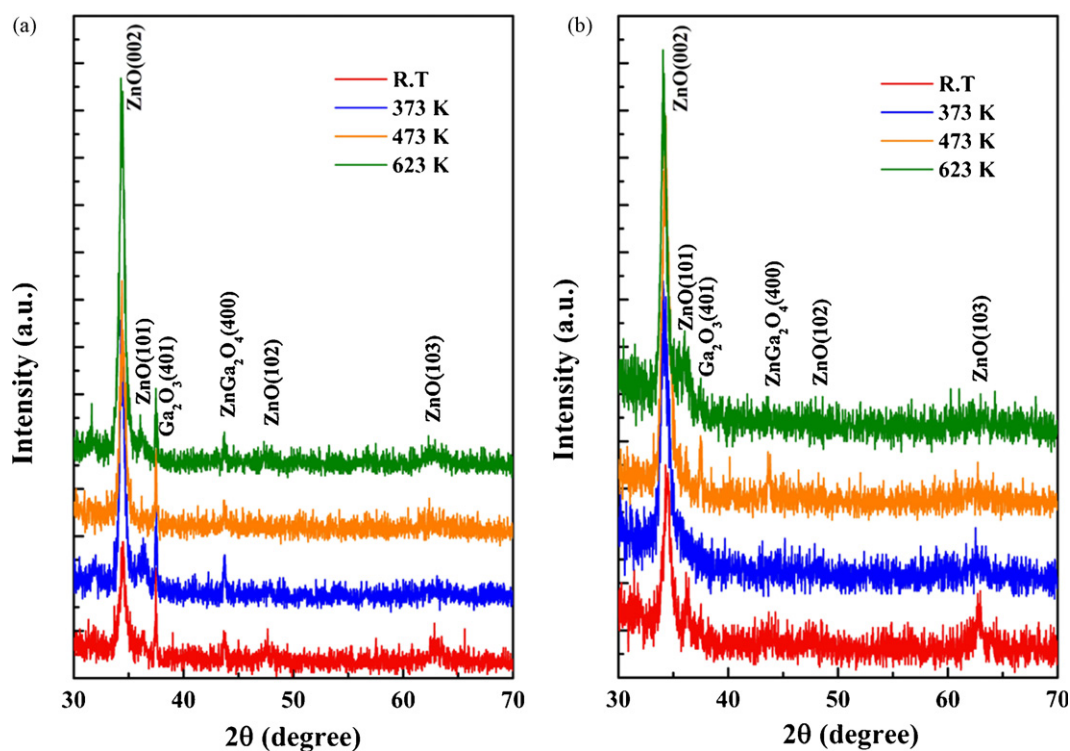


Fig. 3. Comparison of the XRD spectra for the (a) as-deposited and (b) post-annealed ZnO:Ga thin films.

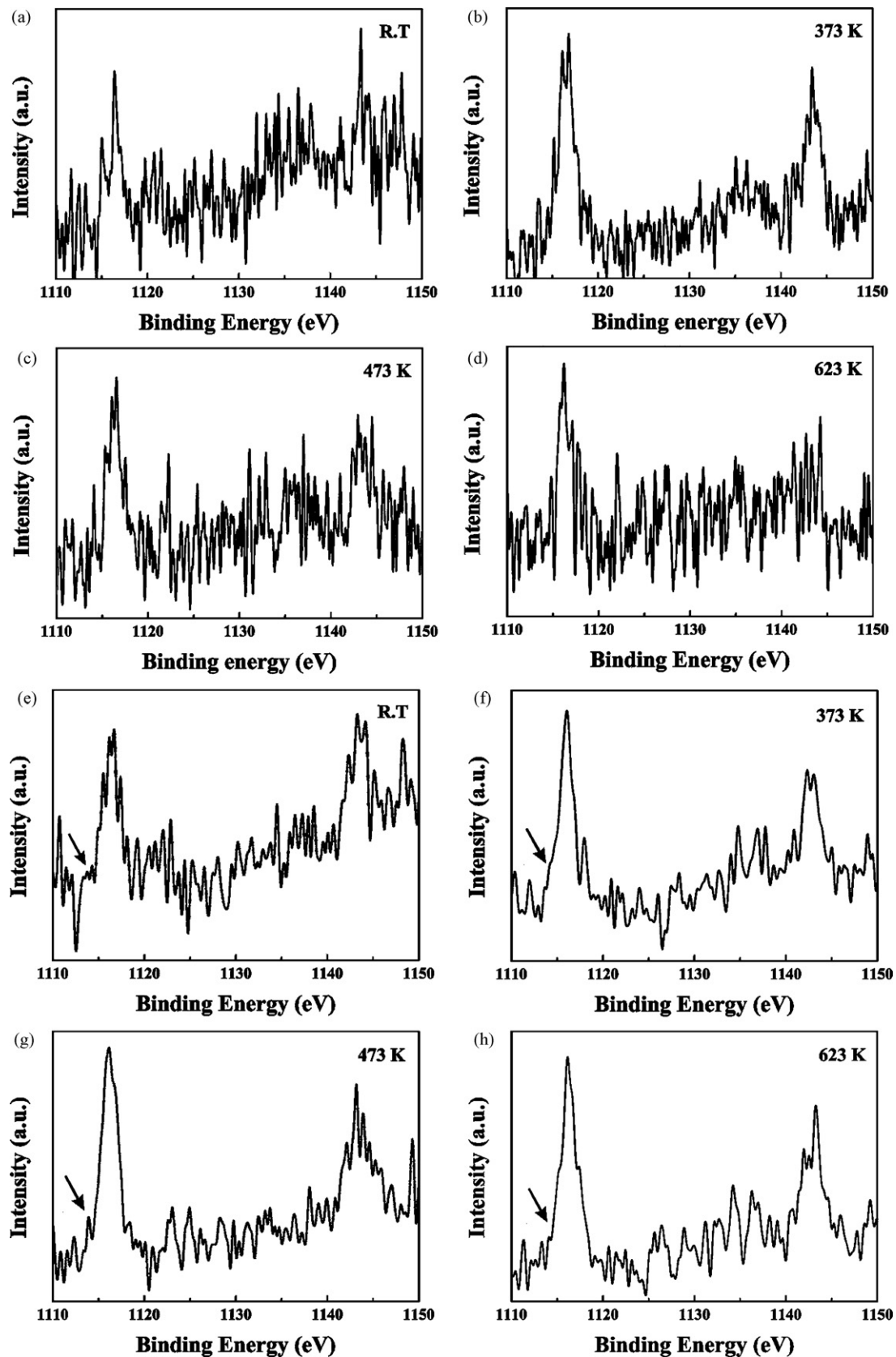


Fig. 4. Changes of the Ga 2p XPS peaks for the (a–d) as-deposited and (e–h) post-annealed ZnO:Ga thin films deposited at various temperatures.

fully incorporated in the ZnO matrix since the Ga concentration is already in excess of the solubility limit.

The microstructural and compositional observations so far are well correlated to the measured electrical properties. Fig. 5(a)

shows the electrical properties of the ZnO:Ga thin films deposited at various temperatures. It is noted that there is some improvement in electrical properties with increasing deposition temperature up to 473 K as represented by the increasing carrier

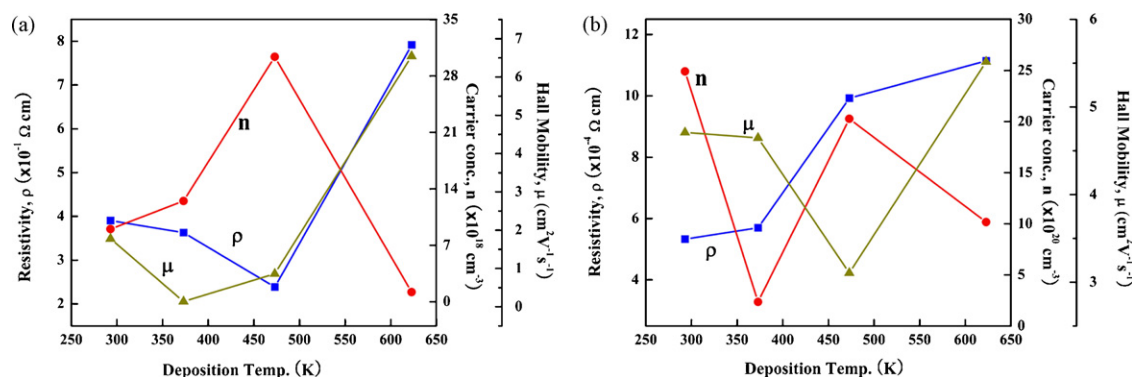


Fig. 5. Changes in the electrical properties of the ZnO:Ga thin films, (a) as-deposited and (b) post-annealed in H₂ ambient, plotted as functions of deposition temperature.

concentration and decreasing resistivity. However, the deposition temperature further increasing to 623 K results in the poorer electrical properties mainly due to the decreasing carrier concentration. Such result is interpreted in following manner. Initially, increasing the deposition temperature improves the crystalline quality and promotes the diffusion of the dopant Ga to the substitutional sites. Especially the latter will contribute to the increased carrier concentration while the former would be related to enhanced carrier mobility. As for the 373 K sample, it is presumed that the decreased mobility resulted since the scattering effect dominated over the crystalline quality effect with increasing carrier concentration. With higher deposition temperature, as mentioned above in the discussion of the XRD spectra, dissociation of Ga₂O₃ and the formation of ZnGa₂O₄ is favored. In this respect, remaining 37.5° peak for the 623 K sample in Fig. 5(a) is interpreted as the peak due to ZnGa₂O₄ (2 2 2) rather than Ga₂O₃ (4 0 1), which is indirectly supported by significantly improved mobility of the 623 K sample, i.e. improved mobility is due to the decomposition of the grain boundary phase Ga₂O₃ acting as the scattering center. Since the Ga atoms in ZnGa₂O₄ is non-substitutional and do not function as the donors, ZnO:Ga thin films deposited at substantially higher temperature would show reduced carrier concentration despite of the increased mobility which is possibly related to the improved crystallinity. In any case, the overall electrical properties of the as-deposited films are poor with their resistivity in the order of $10^{-1} \Omega \text{ cm}$.

After the post-annealing treatment in a H₂ ambient, the electrical properties of the ZnO:Ga thin films in general improved substantially as seen in Fig. 5(b). Now, the resistivity is in the range between mid 10^{-4} and low $10^{-3} \Omega \text{ cm}$ order while it is lower for the samples initially prepared at lower temperatures. It is believed that such decreased resistivity is mainly due to the substantially

increased carrier concentrations to the order of 10^{21} cm^{-3} from 10^{19} cm^{-3} of the as-deposited samples. As for the mobility, it is improved slightly only for the samples deposited at low temperatures (RT and 373 K). Substantial increase in the carrier concentration would be related to the disappearance of the oxide phases in the post-annealed samples [Fig. 3(b)] in the first instance. Further, for the samples initially prepared at RT and 373 K, post-annealing treatment at 623 K could have contributed to the improvement in crystalline quality and to the activation of the dopant Ga. At the same time, as known, the hydrogen annealing ambient could have passivated the negatively charged oxygen species in the grain boundaries and the surfaces which act as carrier traps [27].

In Fig. 5(b), it is noticed that the carrier concentration in general decreases when the deposition temperature is higher. It is also seen that the mobility is more or less similar except for the 473 K sample. It is supposed that decreasing carrier concentration is related to the extent of crystallization of Ga₂O₃ and ZnGa₂O₄ in the as-deposited state. As mentioned above, as the deposition temperature increases, it is likely that crystallinity of these oxide phases increases and this in turn makes their reduction in H₂ ambient more difficult. However, the decrease in carrier concentration is not so significant and it is compensated by the slightly higher mobility with higher deposition temperature due to the improved crystallinity of the films. As a result of this combined effect, overall electrical property remain more or less similar while the sample initially deposited at lower temperature seems to be more advantageous in achieving better electrical properties, e.g. the resistivity as low as about $5.2 \times 10^{-4} \Omega \text{ cm}$.

Another important factor in the consideration of ZnO:Ga thin films as potential TCO is its transmittance to the visible light. In Fig. 6, transmittances of the ZnO:Ga thin films for various

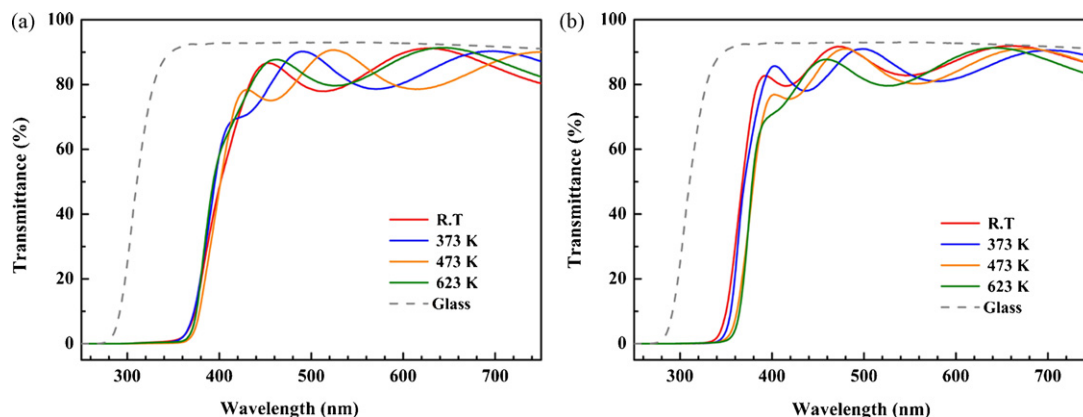


Fig. 6. Changes in the optical properties of the ZnO:Ga thin films, (a) as-deposited and (b) post-annealed in H₂ ambient, plotted as functions of deposition temperature.

wavelengths are compared. In all the wavelength of the visible light, the ZnO:Ga thin films have the relative transmittance over 90% with respect to the glass substrate meaning that these films satisfy basic requirement for the TCO films for display applications. As for the optical band gap, as-deposited films show almost similar value of about 3.35 eV regardless of the deposition temperature [Fig. 6(a)]. On the other hand, after the post-annealing treatment, the optical band gap of the films varies between 3.57 and 3.42 eV depending on the initial deposition temperature [Fig. 6(b)]. The overall increase in the optical band gap after the hydrogen treatment coincides with the increased carrier concentration following the post-annealing in hydrogen while the carrier concentration differs depending on the initial deposition temperature. Therefore, increased optical band gap of the post-annealed ZnO:Ga thin films is believed to be related to Burstein–Moss effect [28], i.e. shifts in the Fermi level due to changes in the concentration of conduction electrons.

4. Conclusions

Structural, electrical and optical properties of ZnO:Ga thin films deposited at various temperatures on glass substrates by RF magnetron co-sputtering were investigated to explore a possibility of producing transparent conductive oxide films through simple low-cost process. It was observed that the ZnO:Ga thin films were grown with *c*-axis preferred orientations without degradation of wurtzite ZnO structure. While undesirable oxide phases such as Ga₂O₃ and ZnGa₂O₄ were formed in the as-deposited films resulting in relatively poor electrical properties, post-annealing treatment in H₂ ambient reduced these phases to release elemental Ga which then acted as dopants. Thus, the resistivity of ZnO:Ga thin films annealed in H₂ ambient at 623 K decreased to the extent of 2–3 orders of magnitude compared to as-deposited thin films. The lowest resistivity of $5.2 \times 10^{-4} \Omega \text{ cm}$ was obtained with the carrier concentration of $2.5 \times 10^{21} \text{ cm}^{-3}$. The values of optical band gap obtained from absorption coefficient vs. $h\nu$ for the annealed thin films were red-shifted and spread out corresponding to activated dopant concentration (carrier concentration), while the values of it for as-deposited thin films were almost identical. This work demonstrates a possibility of producing TCO films based

on ZnO with good electrical and optical properties by simple low-cost process.

Acknowledgement

This work was supported by LG Chem. Ltd. (Grant No. 2007-8-1550).

References

- [1] G.S. Chae, *Jpn. J. Appl. Phys.* 40 (2001) 1282.
- [2] D. Song, A.G. Aberle, J. Xia, *Appl. Surf. Sci.* 195 (2002) 291.
- [3] K. Matsubara, P. Fons, K. Iwata, A. Yamada, K. Sakurai, H. Tampo, S. Niki, *Thin Solid Films* 431–432 (2003) 369.
- [4] F. Zhu, K. Zhang, E. Guenther, C.S. Jin, *Thin Solid Films* 363 (2000) 314.
- [5] H. Kim, J.S. Horwitz, G.P. Kushto, Z.H. Kafafi, D.B. Chrisey, *Appl. Phys. Lett.* 79 (2001) 284.
- [6] O. Bamiduro, H. Mustafa, R. Mundle, R.B. Konda, A.K. Pradhan, *Appl. Phys. Lett.* 90 (2007) 252108.
- [7] B.Z. Dong, G.J. Fang, J.-F. Wang, W.J. Guan, X.Z. Zhao, *J. Appl. Phys.* 101 (2007) 033713.
- [8] T. Minami, H. Nanto, S. Takata, *Jpn. J. Appl. Phys.* 24 (1985) L605.
- [9] Y. Igasaki, H. Saito, *Thin Solid Films* 199 (1991) 223.
- [10] S.Y. Myong, K.S. Lim, *Appl. Phys. Lett.* 82 (2003) 3026.
- [11] V. Assuncao, E. Fortunato, A. Marques, H. Aguiar, I. Ferreira, M.E.V. Costa, R. Martins, *Thin Solid Films* 427 (2003) 401.
- [12] T. Tsuji, M. Hirohashi, *Appl. Surf. Sci.* 157 (2000) 47.
- [13] B.Y. Oh, M.C. Jeong, J.M. Myoung, *Appl. Surf. Sci.* 253 (2007) 7157.
- [14] B.D. Ahn, J.H. Kim, H.S. Kang, C.H. Lee, S.H. Oh, K.W. Kim, G.E. Jang, S.Y. Lee, *Thin Solid Films* 516 (2008) 1382.
- [15] X. Yu, J. Ma, F. Ji, Y. Wang, X. Zhang, C. Cheng, H. Ma, *Appl. Surf. Sci.* 239 (2005) 222.
- [16] V. Bhosle, A. Tiwari, J. Narayan, *J. Appl. Phys.* 100 (2006) 033713.
- [17] R. Al Asmar, S. Juillaguet, M. Ramonda, A. Giani, P. Combette, A. Houry, A. Foucaran, *J. Cryst. Growth* 275 (2005) 512.
- [18] S.M. Park, T. Ikegami, K. Ebihara, *Thin Solid Films* 513 (2006) 90.
- [19] Z.F. Liu, F.K. Shan, Y.X. Li, B.C. Shin, Y.S. Yu, *J. Cryst. Growth* 259 (2003) 130.
- [20] H. Gomez, A. Maldonado, M. de la, L. Olvera, D.R. Acosta, *Sol. Energy Mater. Sol. Cells* 87 (2005) 107.
- [21] S. Zafar, C.S. Ferekides, D.L. Morel, *J. Vac. Sci. Technol. A* 13 (1995) 2177.
- [22] A. Van der Drift, *Philips Res. Rep.* 22 (1967) 267.
- [23] J.A. Sans, A. Segura, J.F. Sánchez-Royo, V. Barber, M.A. Hernández-Fenollosa, B. Marí, *Superlattices Microstruct.* 39 (2006) 282.
- [24] J. Hu, R.G. Gordon, *J. Appl. Phys.* 71 (1992) 880.
- [25] A. de Souza Gonçalves, S.A.M. de Lima, M.R. Davolos, S.G. Antônio, C. de Oliveira Paiva-Santos, *J. Solid State Chem.* 179 (2006) 1330.
- [26] V. Bhosle, A. Tiwari, J. Narayan, *Appl. Phys. Lett.* 88 (2006) 032106.
- [27] S. Kim, J. Jeon, H.W. Kim, J.G. Lee, C. Lee, *Cryst. Res. Technol.* 41 (2006) 1194.
- [28] B.Y. Oh, M.C. Jeong, D.S. Kim, W. Lee, J.M. Myoung, *J. Cryst. Growth* 281 (2005) 475.